Far-infrared spectroscopy of spin excitations and Dzyaloshinskii-Moriya interactions in the Shastry-Sutherland compound SrCu$_2$(BO$_3$)$_2$

T. Rõõm,* D. Hüvonen, and U. Nagel

National Institute of Chemical Physics and Biophysics, Akadeemia tee 23, 12618 Tallinn, Estonia

J. Hwang and T. Timusk

Department of Physics and Astronomy, McMaster University, Hamilton, Ontario L8S4M1, Canada

H. Kageyama

Department of Chemistry, Graduate School of Science, Kyoto University, Kyoto, 606-8502, Japan

We have studied spin excitation spectra in the Shastry-Sutherland model compound SrCu$_2$(BO$_3$)$_2$ in magnetic fields using far-infrared Fourier spectroscopy. The transitions from the ground singlet state to the triplet state at 24 cm^{-1} and to several bound triplet states are induced by the electric field component of the far-infrared light. To explain the light absorption in the spin system we invoke a dynamic Dzyaloshinskii-Moriya (DM) mechanism where light couples to a phonon mode, allowing the DM interaction. Two optical phonons couple light to the singlet to triplet transition in SrCu$_2$(BO$_3$)$_2$. One is a-polarized and creates an intradimer dynamic DM along the c axis. The other is c-polarized and creates an intradimer dynamic DM interaction, it is in the (ab) plane and perpendicular to the dimer axis. Singlet levels at 21.5 and 28.6 cm^{-1} anticross with the first triplet as is seen in far-infrared spectra. We used a cluster of two dimers with a periodic boundary condition to perform a model calculation with scaled intra- and interdimer exchange interactions. Two static DM interactions are sufficient to describe the observed triplet state spectra. The static interdimer DM in the c-direction $d_1 = 0.7$ cm^{-1} splits the triplet state sublevels in zero field [Cépas *et al.*, Phys. Rev. Lett. **87**, 167205 (2001)]. The static intradimer DM in the (ab) plane (perpendicular to the dimer axis) $d_2 = 1.8$ cm^{-1}, allowed by the buckling of CuBO$_3$ planes, couples the triplet state to the 28.6 cm^{-1} singlet as is seen from the avoided crossing.

I. INTRODUCTION

In spin systems with a ground singlet state and excited triplet state the energy gap between the singlet and the triplet can be tuned with an external magnetic field. In SrCu$_2$(BO$_3$)$_2$ it was discovered that in magnetic fields above 22 T, where the spin gap is expected to close, several magnetization plateaus appear.[1] At magnetization plateaus the triplets form a pattern which breaks the translational symmetry of the crystal structure.[2] The heavy mass of the triplet excitations arising from an almost flat dispersion of energy on momentum[3] favors the build-up of magnetic superstructures. Below the critical field SrCu$_2$(BO$_3$)$_2$ has a ground state described first by Shastry and Sutherland.[4]

SrCu$_2$(BO$_3$)$_2$ consists of planes of CuBO$_3$ and Sr atoms between the planes. Cu^{2+} spins ($S=1/2$) form Cu-Cu dimers arranged into orthogonal dimer network. SrCu$_2$(BO$_3$)$_2$ is an experimental realization of a Shastry-Sutherland model.[4] In the model there is an antiferromagnetic intradimer exchange coupling j_1 and interdimer coupling j_2 between spins on the nearest-neighbor dimers (Fig. 1). In the limit of $\alpha \equiv j_2/j_1 = 0$ the problem reduces to that of isolated dimers where the ground state is the product of singlet states and the first excited triplet state is at energy $\Delta_T = j_1$ above the ground state, where Δ_T is the energy per dimer. Shastry and Sutherland showed that for $0 < \alpha \lesssim 0.5$ singlets on all dimers is an exact ground state too. The exactness of the ground state and the

heavy mass of triplet excitations is the consequence of frustration originating from the special geometry of the dimer lattice in the Shastry-Sutherland model where the bonds on neighboring dimers are orthogonal. Later on it has been shown that singlets on all dimers is the exact ground state for a larger range of α up to the quantum critical point $\alpha_c \approx 0.7$. At the quantum critical point the spin gap vanishes and a long-range antiferromagnetic order is established. Different theoretical approaches have been used to calculate α_c (see Ref. 5 for review). It is possible that between the exact singlet ground state and the anti-ferromagnetic state in certain range of α other gapped spin states exist.[6–11]

The singlet-triplet gap in SrCu$_2$(BO$_3$)$_2$, $\Delta_T = 24$ cm^{-1}, has been measured directly by several experimental techniques: inelastic neutron scattering,[3,12] electron spin resonance[13,14] (ESR), Raman scattering,[15] and far-infrared (FIR) spectroscopy.[16] Additional information besides Δ_T is needed to determine the exchange parameters of SrCu$_2$(BO$_3$)$_2$. The dispersion of the triplet excitation is not informative because of its flatness,[3] but positions of other excited states or the temperature dependence of thermodynamic parameters can be used for determining the exchange parameters. Miyahara and Ueda[5] found $j_1 = 59$ cm^{-1} and $\alpha = 0.635$. They added an interlayer coupling $j_3 = 0.09 j_1$ to the model to obtain a better fit of the magnetization T-dependence above the critical temperature $k_B T > \Delta_T$. Based on the analysis of excitation spectra[17] $j_1 = 50$ cm^{-1} and $\alpha = 0.603$ were proposed. Such
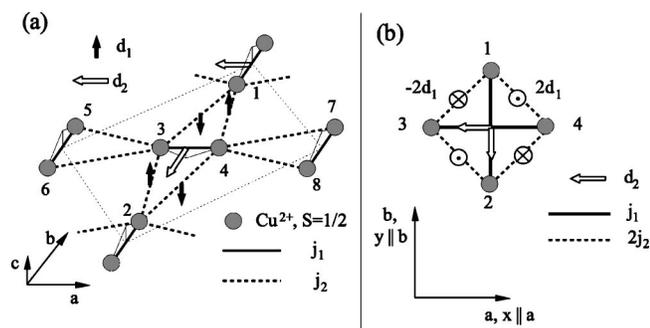
FIG. 1. Cluster with two dimers (1,2) and (3,4). (a) Dimer (3,4) and four nearest-neighbor dimers. The thin dashed line shows the two dimer cluster boundary. Thin solid lines show the distortion of Cu-Cu superexchange bonds due to the buckling of Cu-O-B planes. Thick solid and dashed lines are the inter- and intradimer superexchange constants j_1 and j_2; interdimer DM vectors ($\mathbf{d}_1$, solid arrow) are in the c direction and intradimer DM vectors ($\mathbf{d}_2$, empty arrow) in the (ab) plane along a and b axis. (b) The two dimer model after the periodic boundary condition has been applied; interdimer interactions have doubled.

scattering of parameters could be either due to the incomplete model or due to the approximations made in theoretical calculations. $SrCu_2(BO_3)_2$ is near to the quantum critical point α_c where the energy levels of the spin system are sensitive to the choice of j_1 and α. A singlet level in the spin gap at 21 cm^{-1} found in the ESR spectra[14] may help to find proper parameters for the model.

Interactions other than inter- and intradimer exchange coupling can spoil the exactness of the ground state. This is important in high magnetic fields where the triplet state becomes degenerate with the ground singlet state. At this critical field even a weak interaction between the singlet and the triplet state mixes the two states completely. The singlet and triplet state anticrossing effects were seen in the high field ESR experiments.[14] A possible antisymmetric interaction which couples the singlet and the triplet states is the DM interaction. An intradimer DM is allowed by symmetry but its strength is not known below room temperature. Above room temperature $d_2 = 2.5$ cm^{-1} has been estimated from the ESR linewidth.[18] The interdimer DM interaction, $d_1 = 1.5$ cm^{-1}, perpendicular to the dimer planes[12] partially lifts the degeneracy of the triplet state but does not couple the triplet state to the singlet state. The effect of DM interactions on the magnetic dipole active ESR transitions in $SrCu_2(BO_3)_2$ was investigated theoretically in Ref. 19.

Lattice distortions, static or dynamic, are important in $SrCu_2(BO_3)_2$ since they lower the crystal symmetry and allow magnetic interactions which are otherwise forbidden in a more symmetric environment. $SrCu_2(BO_3)_2$ has a structural phase transition at 395 K (Ref. 20) that induces a buckling of $CuBO_3$ planes in the low T phase. As the phase transition point is approached from below the Raman-active 62 cm^{-1} optical phonon mode softens.[21] Acoustic phonon modes have spin-phonon coupling at magnetization plateaus.[22] It has been proposed that a spin superstructure at 1/8 plateau observed by nuclear magnetic resonance at 35 mK is stabilized by a lattice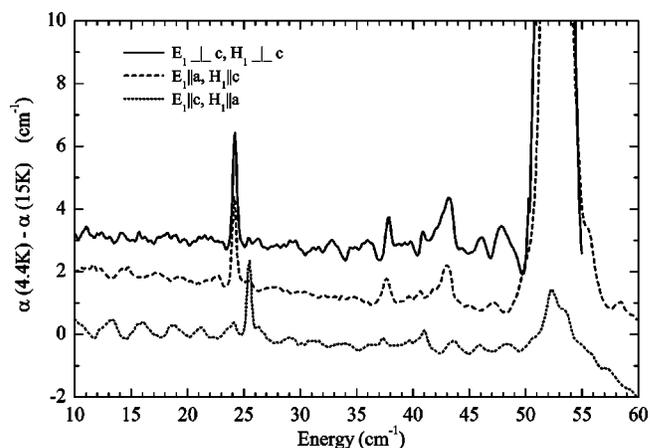 distortion.[2] Instantaneous breaking of lattice symmetry by an optical phonon allows electric dipole active singlet-triplet transitions[23] that explains FIR polarized absorption spectra in $SrCu_2(BO_3)_2$.[16]

Our aim is to find out which additional interactions are required to the Shastry-Sutherland model that add triplet corrections to the ground state. For that we do FIR absorption measurements with polarized light in magnetic field and compare the absorption line frequencies and intensities with values calculated with a two dimer model including the dynamic DM effect. The important information is in the polarization and magnetic field dependence of the FIR absorption lines and in the avoided crossing effects.

We studied single crystals of $SrCu_2(BO_3)_2$, Ref. 24. The first sample consisted of two pieces 0.65 mm thick in the a-direction with the total area of 12 mm^2 in the (ac) plane. The second sample was 0.6 mm thick in the c-direction and had an area of 11.5 mm^2 in the (ab) plane. The experimental details are described in Refs. 16 and 25.

FIG. 2. Differential absorption in $\mathbf{E}_1 \perp \mathbf{c}$ (two upper curves) and $\mathbf{E}_1 \| \mathbf{c}$ (lower curve) polarization. Spectra have been offset in the vertical direction.

II. RESULTS AND DISCUSSION

A. FIR spectra and electric dipole transitions

As the result of the polarization sensitive measurement of FIR spectra we have identified that the main resonances in the spectra are electric dipole transitions, rather than being magnetic dipole transitions. In Fig. 2 differential absorption spectra at 4.4 K relative to 15 K, are displayed. The strong absorption lines at 52.3 and 53.5 cm^{-1} were identified[16] as electric dipole transitions, that are active in $\mathbf{E}_1 \| \mathbf{a}$ polarization. We see the same for the 43.0 cm^{-1} singlet and T_0 and T_1 triplets (see Table I) at 24.2 and 37.5 cm^{-1}, respectively, which are present in the spectra measured with $\mathbf{E}_1 \| \mathbf{a}$ regardless of $\mathbf{H}_1$ being perpendicular to the c axis or parallel to it. The lines are missing in $\mathbf{E}_1 \| \mathbf{c}$ polarization,[26] instead a new line appears at 25.5 cm^{-1}, which is identified as another component of the triplet T_0.

The triplets are split by the magnetic field $\mathbf{B}_0$. Differential absorption spectra in $\mathbf{E}_1 \| \mathbf{a}$ polarization for one magnetic field direction, $\mathbf{B}_0 \| \mathbf{a}$, measured relative to the zero field, are

TABLE I. Singlet and triplet excitations observed in the FIR spectra at 4.4 K in the order of increasing zero field energies $\hbar\omega_0$ (in cm^{-1} units). When a line is visible in two $\mathbf{E}_1$ polarizations, both are indicated. The corresponding $\mathbf{H}_1$ polarizations are also indicated. S and T label the singlet and triplet states; $+$ $(-)$ denotes levels which energy increases (decreases) with $\mathbf{B}_0$ and 0 indicates levels where the energy stays constant; g_a and g_c are the g-factors with $\mathbf{B}_0 \| \mathbf{a}$ and $\mathbf{B}_0 \| \mathbf{c}$, respectively. The labeling of T_0 levels is shown in Fig. 5. The zero field intensities A_0 (in cm^{-2} units) of T_0 ($\star$) are described in the text and in Figs. 4–6. High energy excitations are labeled by their energies.

| Label	$\mathbf{E}_1$	$\mathbf{H}_1$	A_0	$\hbar\omega_0$	g_a	g_c
S_1	a	c		21.50±0.03		
$T_{0m}(\pm)$	a,c	c,a	$\star$	22.72±0.05	1.988	2.219
$T_{0p,m}(0)$	a,c	c,a	$\star$	24.11±0.05		
$T_{0p}(\pm)$	a,c	c,a	$\star$	25.51±0.05	1.988	2.219
S_2	a,c	c,a		28.57±0.03		
$T_1(\pm)$	c	a	0.3±0.2	37.49±0.03	1.996	2.264
$T_1(\pm)$	a	b,c	0.9±0.2	37.51±0.04	2.001	2.23
$T_1(0)$	a	c	0.9±0.2	37.69±0.09		
$T_{38.7}(\pm)$	a	c		38.74±0.03	2.026	
$T_{38.7}(0)$	c	a		38.70±0.15		
$T_{39.1}(\pm)$	c	a		39.08±0.15	2.067	2.29
$S_{39.7}$	a	c	0.19±0.05	39.71±0.04		
$T_{40.5}(\pm)$	a	c		40.45±0.03	1.97	
$T_{40.7}(\pm)$	c	a	0.2±0.1	40.67±0.03		2.243
$T_{40.7}(0)$	a,c	c,a	0.2±0.1	40.70±0.16		
$T_{41.1}(\ )$	c	a	0.4±0.1	41.11±0.13	2.10	
$T_{42.7}(+)$	a	c	0.2±0.1	42.7±0.2		2.25
S_{43}	a	b,c	2.6±0.3	43.00±0.16		
$T_{43.5}(\pm)$	c	a	0.2±0.1	43.54±0.03		2.31
$S_{44.7}$	c	a		44.7±0.4		
$S_{47.0}$	c	a		47.04±0.04		
$T_{48.2}(\pm)$	c	a	0.04±0.02	48.21±0.09		2.27
$S_{52.3}$	a	b,c	86±14	52.24±0.08		
$S_{53.5}$	a	b,c	24±3	53.44±0.07		
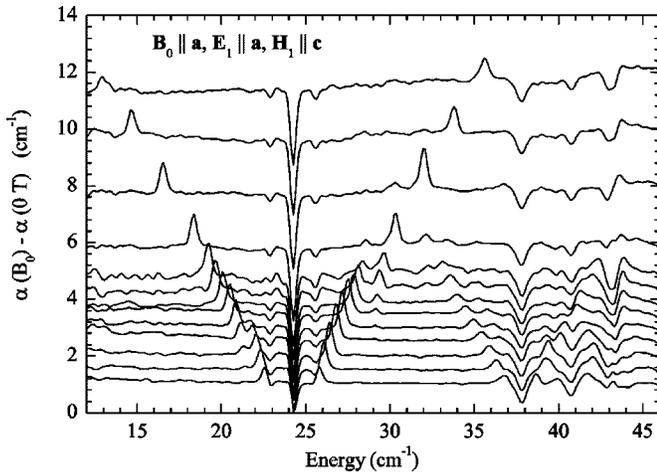
FIG. 3. Differential absorption spectra in magnetic field $\mathbf{B}_0 \| \mathbf{a}$ at 4.4 K. Vertical offset equals the magnetic field value in Tesla.

displayed in Fig. 3. We see an anticrossing of the $T_{0m}(-)$ level with the singlet S_1 at 21.5 cm^{-1} and an anticrossing of the $T_{0p}(+)$ level with the singlet S_2 at 28.6 cm^{-1}. All the peaks in the measured spectra in different light polarizations and $\mathbf{B}_0$ directions were fitted with Lorentzians. The results are summarized in Table I and displayed in Figs. 4–6. The states above 38 cm^{-1} are labeled by their zero field frequencies. The magnetic field independent energy levels are labeled as singlets with the exception of those in the middle of the triplet levels $T(\pm)$.

B. Dynamic Dzyaloshinskii-Moriya mechanism and optical transitions: Two dimers

The Hamiltonian for a spin pair with exchange coupling j and DM interaction $\mathbf{d}$ on the bond connecting spins k and l reads
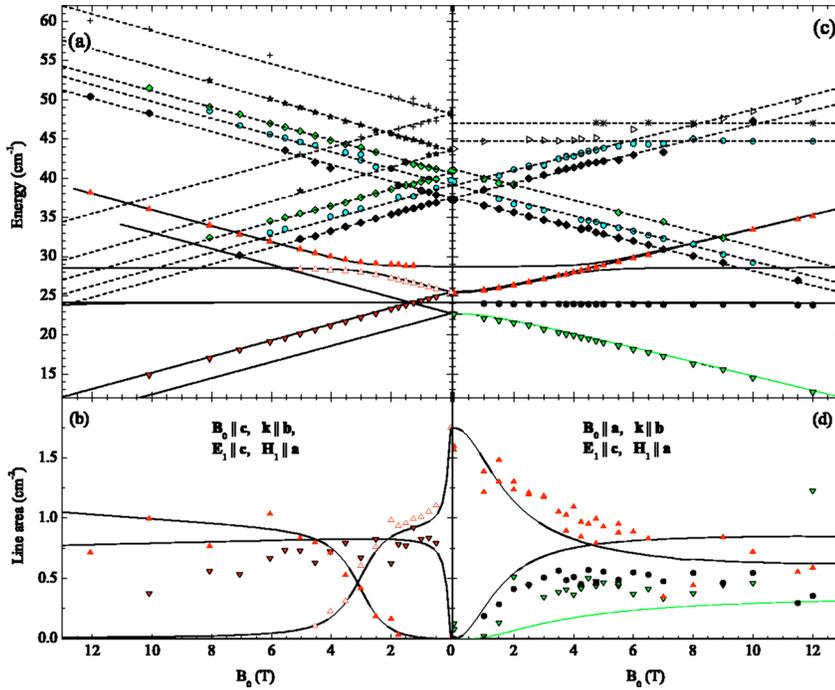
FIG. 4. (Color online) Magnetic field dependence of line positions and line areas in $\mathbf{E}_1 \| \mathbf{c}$ polarization at 4.4 K; (a), (b) $\mathbf{B}_0 \| \mathbf{c}$; (c), (d) $\mathbf{B}_0 \| \mathbf{a}$. Solid lines are the results of the calculation based on the two dimer model: $j_1 = 24$ cm^{-1}, $2j_2 = 9.8$ cm^{-1}, $2d_1 = 1.4$ cm^{-1}, and $d_2 = 1.8$ cm^{-1}. Dashed lines in panels (a) and (c) are fits with parameters given in Table I.

$$H_{\text{stat}}^{kl} = \left(j - \frac{|\mathbf{d}|^2}{4j} \right) \mathbf{S}_k \cdot \mathbf{S}_l + \frac{1}{2j} \mathbf{S}_k \cdot \mathbf{dd} \cdot \mathbf{S}_l + \mathbf{d} \cdot [\mathbf{S}_k \times \mathbf{S}_l]$$

$$+ g\mu_B \mathbf{B}_0 \cdot (\mathbf{S}_k + \mathbf{S}_l). \tag{1}$$

Here we included Shekhtman corrections[27,28] which are quadratic in $\mathbf{d}$ (see also Ref. 25). The last term is the Zeeman energy of spins in the magnetic field $\mathbf{B}_0$ where g is the electron spin g-factor and μ_B is the Bohr magneton.

The formalism to introduce the spin-phonon coupling is similar to one used in Refs. 23 and 25. We are interested in singlet to triplet transitions. Therefore the relevant term is the antisymmetric DM interaction $\mathbf{d}(Q) \cdot [\mathbf{S}_k \times \mathbf{S}_l]$ which couples the singlet to the triplet state. We expand the DM vector $\mathbf{d}(Q)$ into a power series of the lattice normal coordinate Q

$$\mathbf{d}(Q) = \mathbf{d}(0) + \left. \frac{\partial \mathbf{d}}{\partial Q} \right|_{Q=0} Q + \ldots, \tag{2}$$

where $\mathbf{d}(0) \equiv \mathbf{d}$ is the static DM interaction in (1). We keep terms linear in Q. The full Hamiltonian for a spin pair including the phonons is

$$H^{kl} = H_{\text{stat}}^{kl} + \hbar\omega_p a^\dagger a + q(a^\dagger + a)\mathbf{d}_Q \cdot [\mathbf{S}_k \times \mathbf{S}_l], \tag{3}$$

where $\mathbf{d}_Q \equiv \partial\mathbf{d}/\partial Q|_{Q=0}$. The lattice normal coordinate Q is presented in terms of phonon creation and annihilation operators $a^\dagger$ and a, $Q = q(a^\dagger + a)$, where q is the transformation coefficient and ω_p is the phonon frequency. The spin-phonon coupling term in (3) is linear in $a^\dagger$ and a. Therefore the phonon states with the occupation numbers n and n' are coupled where $n' = n \pm 1$. We will consider only two phonon states $|0\rangle$ and $|1\rangle$, which is justified when $k_B T \ll \hbar\omega_p$.

The normal coordinate Q in the dynamic DM singlet to triplet optical transition mechanism belongs to an optical phonon. Electric dipole coupling between a phonon and light in the long wavelength limit is

$$V = eQE_1 = eq(a^\dagger + a)E_1, \tag{4}$$

where e is the effective charge associated with the lattice normal coordinate Q. Here we assumed $\mathbf{E}_1 \| \mathbf{Q}$ and dropped the time dependence of V. Once the eigenstates of (3) are known the optical transition probability between the ground state $|\phi\rangle$ and the excited state $|\phi'\rangle$ is calculated as $I = |\langle\phi'|V|\phi\rangle|^2$.

To calculate optical transitions in SrCu$_2$(BO$_3$)$_2$ we use a two dimer model depicted in Fig. 1. In this model intradimer and interdimer superexchange interactions j_1 and j_2 are considered. The interdimer static DM vector $\mathbf{d}_1$ is along the c axis and alternates from bond to bond. The intradimer static DM vector $\mathbf{d}_2$ exists due to the buckling of Cu-O-B planes.[20] The direction of DM vectors is defined by the right-hand rule where the path is along the Cu-O-Cu bond (for $\mathbf{d}_1$ Cu-O-B-O-Cu) in the direction of increasing spin index k. In the vector product $\mathbf{S}_k \times \mathbf{S}_l$ the spin with a smaller index is on the left, $k < l$. When a periodic boundary condition is applied to the two dimer cluster, bounded by a box drawn with a thin dashed line in Fig. 1(a), an effective spin model is obtained where the interdimer interactions are doubled, Fig. 1(b). The doubling is necessary to conserve the number of next-nearest-neighbor bonds, which is four.

The Hamiltonian for the two dimer cluster is the sum of pairwise interactions (3) where the sum runs over all the bonds in the cluster. We will use a basis $|ABn\rangle$, where A runs over the singlet S and three triplet components T_-, T_0, and T_+ on the j_1 bond of the dimer (1,2) and B over the singlet and triplet states of the dimer (3,4). n is the number of phonons, 0 or 1. The basis has 32 components. Below we consider a- and c-axis phonons, shown in Fig. 7, named by the direction of their electric dipole moment.

1. Energy levels

The effect of the dynamic DM interaction on the position of energy levels is small because we take $\hbar\omega_p = 100$ cm^{-1}
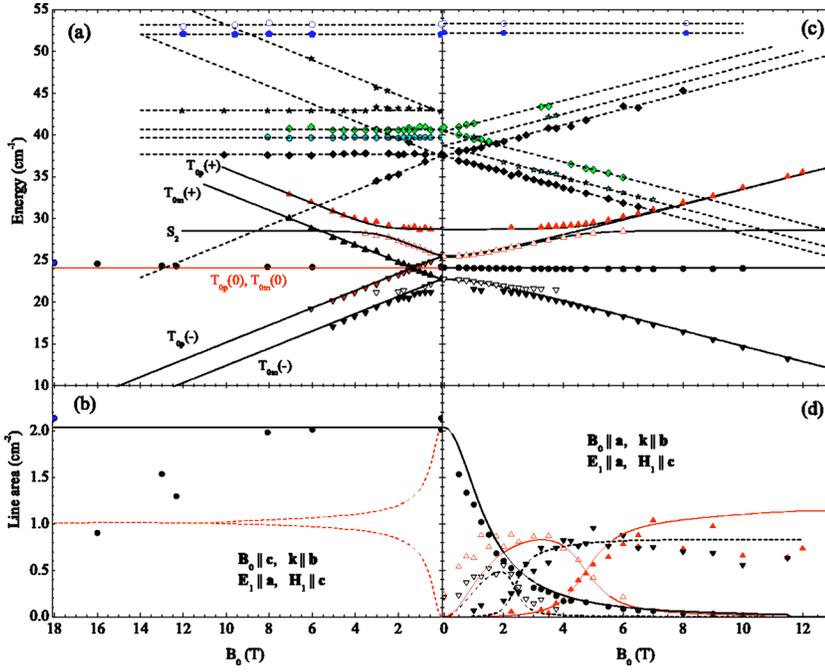
FIG. 5. (Color online) Magnetic field dependence of line positions and line areas in $\mathbf{E}_1 \| \mathbf{a}$ polarization at 4.4 K; (a), (b) $\mathbf{B}_0 \| \mathbf{c}$; (c), (d) $\mathbf{B}_0 \| \mathbf{a}$. Solid lines are the results of the calculation based on the two dimer model: $j_1 = 24$ cm^{-1}, $2j_2 = 9.8$ cm^{-1}, $2d_1 = 1.4$ cm^{-1}, and $d_2 = 1.8$ cm^{-1}. Dashed lines in panels (a) and (c) are fits with parameters given in Table I. The solid line in panel (b) is the sum of two theoretical line areas of S_0 to $T_{0m}(0)$ and to $T_{0p}(0)$ transitions shown by dashed lines. Dashed lines in (d) are eye guides (see text). The 18 T point a panels (a) and (b) was measured at 1.8 K.

that is substantially larger than the singlet-triplet gap. We use this value since there are no optical phonons with substantial spectral weight below 100 cm^{-1} as our transmission measurements show. The energy spectrum can be analyzed separately from the dynamic DM effect because of the high phonon energy. The calculated energy levels are the same in Figs. 4 and 5. In these figures only the zero phonon levels of the triplet T_0 and S_2 are shown. The levels with one excited phonon are offset by $\hbar \omega_p$ to higher energies and are not shown.

In a two dimer system two singlets, two triplets, and a quintet are present. The ground state is a product of singlets $|SS\rangle$. The first triplet is a linear combination of $|ST\rangle$ and $|TS\rangle$. In the two dimer model the singlet-triplet splitting is not renormalized by the interdimer coupling j_2 and the energy of the triplet excitation is $E_{T0} = j_1$. The second singlet, a bound state of two triplets, is at $E_{S1} = 2j_1 - 2(2j_2)$. To stress the fact that in the two dimer model with a periodic boundary condition the interdimer bonds are effectively doubled, we write $2j_2$ explicitly. There are two other bound states of two triplets, a triplet at $E_{T1} = 2j_1 - (2j_2)$ and a quintet at $E_Q = 2j_1 + (2j_2)$. These energies and the ground state wave function are slightly changed by the static DM interactions d_1 and d_2. The spin states $|ST_i\rangle$ and $|T_iS\rangle$ are strongly mixed by the interdimer d_1 since they are degenerate in any field.

The states are labeled in Fig. 5. The following parameters were used to fit the energy spectra plotted in Figs. 4 and 5. The energy of one-triplet sublevels $T_{0m}(0)$ and $T_{0p}(0)$ gives us $j_1 = 24.0$ cm^{-1}. To get the singlet S_2 at 28.6 cm^{-1} we use $2j_2 = 9.8$ cm^{-1}. Triplet levels are split in zero field by $2d_1 = 1.4$ cm^{-1}. The intradimer $d_2 = 1.8$ cm^{-1} induces an avoided crossing of $T_{0p}(+)$ and S_2. In a simplified picture the one-triplet excitation is the $|ST\rangle$ (or $|TS\rangle$) state and the excited singlet is $|TT\rangle$. d_2 "flips" the singlet to the triplet state on one of the dimers and thus couples $T_{0p}(+)$ to S_2.

2. c-axis phonon

The optical c-axis phonon bends the Cu-O-Cu bond in the c-direction. We assume that the bending action of the phonon is the same on both dimers, Fig. 7. As a result the dynamic DM interaction on the dimer (1,2) is $q_c \mathbf{d}_{Q_c} \equiv \mathbf{d}_{3c} = (-d_{3c}, 0, 0)$ and on the dimer (3,4) $\mathbf{d}_{3c} = (0, d_{3c}, 0)$; the orientation of the Cartesian coordinates is the same as in Fig. 1(b). The calculated and the measured transition probabilities as a function of magnetic field are plotted in Figs. 4(b) and 4(d) for two field orientations. In zero field a line at 25.5 cm^{-1} is present. The area of this line is the only scaling parameter between the theory and the experiment. Note that the transition to the triplet level, which anticrosses with S_2, is optically active when $\mathbf{B}_0 \| \mathbf{c}$. When $\mathbf{B}_0 \| \mathbf{a}$ there is no anticrossing for the optically active triplet level.

The overall agreement between the theory and the experiment is good. There is a disagreement between the intensities of the middle and lower triplet components in the theory and in the experiment, Fig. 4(d). In the theory the intensity of the middle component is approximately three times as strong as the lower component while in the experiment they are equal. We tried several changes in our model to make the intensities of the two triplet components more equal and none of them helped. These unfruitful changes were the shift of the phonon frequency, a small out-of-plane component of $\mathbf{B}_0$ and an in-plane component of the interdimer DM vector $\mathbf{d}_1$.

3. a-axis phonon

The optical a-axis phonon bends the Cu-O-Cu bond in the a-direction and creates a dynamic DM interaction in the c-direction, Fig. 7. If we choose $\mathbf{E}_1 \| \mathbf{a}$ the dynamic DM interaction is created on dimer (1,2), $q_a \mathbf{d}_{Q_a} \equiv \mathbf{d}_{3a} = (0, 0, d_{3a})$. In general, for an arbitrary orientation of $\mathbf{E}_1$ in the (ab) plane, both dimers will acquire a certain $\mathbf{d}_{3a}$. For the time being we assume $\mathbf{E}_1 \| \mathbf{a}$.
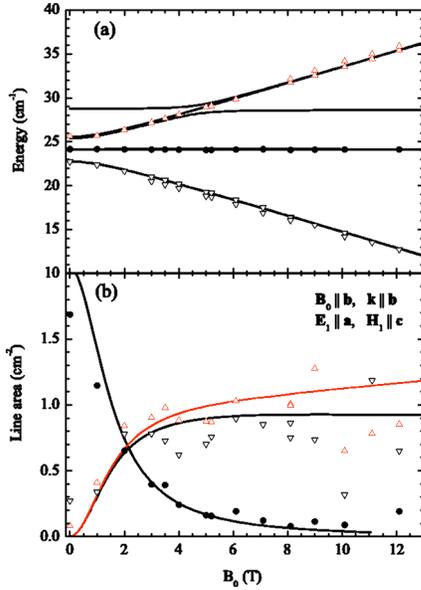
FIG. 6. (Color online) Line positions (a) and line areas (b) in $\mathbf{E}_1 \| \mathbf{a}$ and $\mathbf{B}_0 \| \mathbf{b}$ configuration at 4.4 K. The lines are results of the calculation based on the two dimer model and dynamic DM interaction. The additional splitting of triplet components (triangles) is caused by the magnetic field $\mathbf{B}_0$ being misaligned by 9° out of the (*ab*) plane (Ref. 26). In panel (b) the line area (triangles up or triangles down) is a sum of line areas of split components.

In zero magnetic field the transition to the central triplet component is observed, Fig. 2. As the $\mathbf{B}_0 \| \mathbf{c}$ field is turned on, Fig. 5(b), the central line, being a sum of two overlapping transitions, conserves its intensity. The experimentally observed drop in intensity with increasing field is a T effect. At 1.8 K (18 T field) the intensity is recovered. Besides the strong central line there are in zero field two sidepeaks ten times weaker at 22.7 and 25.5 cm^{-1} corresponding to transitions to the twice degenerate states $T_{0m}(\pm)$ and $T_{0p}(\pm)$. The dynamic DM interactions due to the a- and c-axis phonons in this $\mathbf{B}_0$ orientation give zero intensity for the sidepeaks. The detailed analysis of the mechanism causing these weak transitions is difficult because in other polarizations and field orientations stronger mechanisms are prevailing. The sidepeaks split in the magnetic field and an avoided crossing with S_1 and S_2 is seen in the experiment.

When the magnetic field is in the (*ab*) plane two cases must be considered, $\mathbf{B}_0 \| \mathbf{E}_1$ and $\mathbf{B}_0 \perp \mathbf{E}_1$. In Figs. 5(c) and
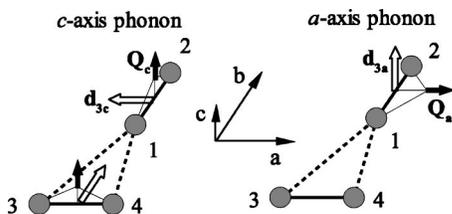

FIG. 7. Intradimer dynamic DM interactions. A lattice distortion with the normal coordinate $\mathbf{Q}$ (solid arrow) creates an intradimer DM interaction $\mathbf{d}_3$ (empty arrow). The c-axis phonon creates a dynamic DM interaction on both dimers while the a-axis phonon affects the dimer (1,2) only.

5(d) the $\mathbf{B}_0 \| \mathbf{E}_1$ case is shown. Here are optically active the triplet levels which anticross with the singlet states. In $\mathbf{B}_0 \perp \mathbf{E}_1$ field orientation, Fig. 6, the optically active triplet levels do not anticross with the singlet states. The mutual orientation of $\mathbf{B}_0$ and $\mathbf{E}_1$ is important because $\mathbf{E}_1 \| \mathbf{a}$ creates $\mathbf{d}_{3a}$ on the dimer (1,2) and not on (3,4). Which set of the twofold degenerate triplet levels is optically active depends on the relative orientation of $\mathbf{B}_0$ and $\mathbf{d}_2$ on the dimer where $d_{3a} \neq 0$. In Fig. 5, $\mathbf{B}_0 \| \mathbf{d}_2$ and in Fig. 6, $\mathbf{B}_0 \perp \mathbf{d}_2$. An additional splitting of $T_{0m}(\pm)$ and $T_{0p}(\pm)$ by 0.6 cm^{-1} seen in Fig. 6 is because $\mathbf{B}_0$ is out of (*ab*) plane by 9°.

C. Static and dynamic DM in SrCu$_2$(BO$_3$)$_2$

We have shown that the first triplet state energy spectra are well described with two static DM interactions, $\mathbf{d}_1$ and $\mathbf{d}_2$. The information about $\mathbf{d}_1$ and $\mathbf{d}_2$ is contained in the position of energy levels and in the FIR absorption line intensities. The interdimer $\mathbf{d}_1$ determines the magnetic field dependence of intensities and the triplet state level energy splitting. The intradimer $\mathbf{d}_2$ determines the extent of the avoided crossing with S_2 and the magnetic field dependence of intensities near the avoided crossing points. Over the magnetic field range of our experiment the intensities of the singlet-triplet absorption lines do not depend on the dynamic part of the DM interaction, because the phonon energies are large compared to the triplet state energy.

Other inter- and intradimer DM interaction components besides $\mathbf{d}_1$ and $\mathbf{d}_2$ have been considered to describe experimental data.[18,29] These are the in-plane component of the interdimer DM $\mathbf{d}_{xy}$ and the symmetry-forbidden intradimer DM $\mathbf{d}_z$ in the c-direction. We included $\mathbf{d}_{xy}$ and $\mathbf{d}_z$ in the two dimer model and found that calculations with nonzero $\mathbf{d}_{xy}$ and $\mathbf{d}_z$ give results contradicting with the experiment. Our argument, which is independent of whether a particular infrared transition is allowed or forbidden, relies on the observed and calculated crossing-anticrossing effects between the triplet and the singlet states.

If $\mathbf{B}_0 \| \mathbf{c}$ and $\mathbf{d}_{xy} \neq 0$ then $T_{0m}(+)$ would have an avoided crossing with S_2 contradicting the experiment, where $T_{0p}(+)$ anticrosses with the singlet [Fig. 5(a)]. Also $\mathbf{d}_z$ does not give any anticrossing between S_2 and $T_{0m}(+)$ or $T_{0p}(+)$. In high field nonzero $\mathbf{d}_2$ creates an avoided crossing between the ground state S_0 and the triplet branch $T_{0m}(-)$ as observed in the experiment[14] while nonzero $\mathbf{d}_{xy}$ or $\mathbf{d}_z$ do not create an avoided crossing between S_0 and $T_{0m}(-)$ or $T_{0p}(-)$. However, the two dimer model does not predict the experimentally observed[14] avoided crossing between S_0 and $T_{0p}(-)$.

In $\mathbf{B}_0 \| \mathbf{a}$ field orientation both $\mathbf{d}_{xy}$ and $\mathbf{d}_z$ add, in addition to $\mathbf{d}_2$, to the avoided crossing of one of the triplet components with S_2. The experimental data can be fitted with a single value $d_2 = 1.8$ cm^{-1} in both field orientations, $\mathbf{B}_0 \| \mathbf{a}$ and $\mathbf{B}_0 \| \mathbf{c}$. If $\mathbf{d}_{xy}$ and $\mathbf{d}_z$ were comparable in magnitude to $\mathbf{d}_2$, then the extent of avoided crossing would be different in $\mathbf{B}_0 \| \mathbf{a}$ and $\mathbf{B}_0 \| \mathbf{c}$ field orientations.

Our conclusion is that the dominant DM interactions are $d_1 = 0.7$ cm^{-1} and $d_2 = 1.8$ cm^{-1}. In the magnetization plateau state the lattice parameters of SrCu$_2$(BO$_3$)$_2$ may change due to spin-phonon coupling.[22] Our calculation of energy levels

did not account for static lattice distortions and therefore we cannot make any conclusions about $\mathbf{d}_{xy}$ and $\mathbf{d}_z$ and the strength of $\mathbf{d}_1$ and $\mathbf{d}_2$ in high magnetic fields.

The intensity of the FIR singlet-triplet transitions depends on the strength of the dynamic DM and on the frequency and the oscillator strength of the phonon. Since the particular phonons involved in the dynamic DM effect in $SrCu_2(BO_3)_2$ are not known we can give only the relative strength of dynamic DM interactions. The a- and c-polarized singlet-triplet transitions have similar oscillator strengths. These are 2.0 cm^{-2} ($\mathbf{E}_1\|\mathbf{a}$) and 1.7 cm^{-2} ($\mathbf{E}_1\|\mathbf{c}$) if we compare the two lower spectra in Fig. 2 which have been measured on the same sample by changing the direction of the light polarization. The ratio of the dynamic DM interactions for the two mechanisms is $d_{3a}/d_{3c}=\sqrt{2\times 2.0/1.7}=1.5$ if we assume that a- and c-axis phonons have equal frequencies and oscillator strengths. The factor 2 accounts for the a-axis phonon creating a dynamic DM only on the dimer with its axis perpendicular to $\mathbf{E}_1$.

D. Staggered *g*-tensor

The importance of the staggered g-tensor in $SrCu_2(BO_3)_2$ was pointed out by Miyahara *et al.*[30] The staggered g-tensor exists in $SrCu_2(BO_3)_2$ because of the buckling of Cu-O-B planes below 395 K. It mixes singlet and triplet states similar to the static DM interaction $\mathbf{d}_2$. The strength of the staggered g-tensor interaction can be estimated and we show that its effect on the energy of the spin levels is small compared with the effect of $\mathbf{d}_2$. The Zeeman term H_{Zs} couples singlet and triplet states on a single dimer and is proportional to $g_s\mu_B B_0$, where $g_s=(g_{\bar{x}}-g_{\bar{z}})\sin\phi\cos\phi$ (Ref. 30). The angle $\phi\approx 6°$ is the buckling angle of the Cu-O-B plane.[20] The components $g_{\bar{x}}$ and $g_{\bar{z}}$ of the Cu ion g-tensor are not known but we take $g_{\bar{x}}\approx g_a=1.998$ and $g_{\bar{z}}\approx g_c=2.219$ (Table I) and get $g_s=0.023$. The staggered term H_{Zs} increases linearly with magnetic field. The largest field where the anticrossing between T_0 and S_2 takes place is 5 T. In this field the magnitude of the staggered g-tensor term in the Hamiltonian is 0.05 cm^{-1}, which is much smaller than the static intradimer DM term $d_2=1.8$ cm^{-1}. We conclude that the dominant coupling between the singlet and the triplet is due to the static DM interaction $\mathbf{d}_2$.

E. States of bound triplets

Several states besides the one-triplet excitation are infrared-active (Table I). We showed that the two dimer model explains well the energies of the one-triplet states and transitions to them. In the two dimer model with $j_1=24$ cm^{-1} and $2j_2=9.8$ cm^{-1} we get several two triplet states: a singlet, a triplet, and a quintet of two bound triplets at 28.4, 38.2, and 57.8 cm^{-1}, respectively.

$SrCu_2(BO_3)_2$ has two low energy singlet states S_1 and S_2 which both anticross with triplet state levels (Figs. 4 and 5). In the two dimer model only one singlet of bound triplets is possible and the anticrossing occurs only with $T_{0p}(\pm)$ states. In the experiment an anticrossing is observed between S_2 and $T_{0p}(+)$, Fig. 5(a). The observed anticrossing between S_1 and

$T_{0m}(-)$ cannot be explained by the two dimer model. In Sec. II C we show that other DM interactions besides $\mathbf{d}_2$ are weak or absent in $SrCu_2(BO_3)_2$ in the studied $\mathbf{B}_0$ range, although they may have proper symmetry to couple S_1 and $T_{0m}(-)$.

The energy of the 38.2 cm^{-1} triplet in the two dimer model is in the range where triplets are present in $SrCu_2(BO_3)_2$. There is a triplet at 37.5 cm^{-1} labeled as T_1 (Table I). FIR transitions to this state are active in $\mathbf{E}_1\|a$ polarization, Fig. 2. In $\mathbf{E}_1\|c$ the transitions are weaker (Table I). The $T_1(0)$ level is FIR active when $\mathbf{B}_0\|c$ and $T_1(\pm)$ are active when $\mathbf{B}_0\perp c$. All this, polarization and magnetic field dependence, is consistent with the dynamic DM mechanism of the FIR absorption where the dynamic DM is along the c axis. The a-axis phonon creates a dynamic DM in the direction parallel to the c axis. The intradimer dynamic DM interaction d_{3a} does not give any transitions to bound states of triplets. We considered a possibility that the a-axis phonon modulates the static interdimer $\mathbf{d}_1$. We found that the pattern of dynamic interdimer DM vectors with the same symmetry as $\mathbf{d}_1$ [Fig. 1(b)] gives selection rules that apply to the 37.5 cm^{-1} T_1 triplet. Transitions to other states are forbidden in the first order of this dynamic DM interaction. The lattice deformation that creates such a pattern of dynamic DM vectors is of A_1 symmetry and is not an optical phonon; in the A_1 symmetry mode Cu atoms on j_1 bond move along the bond in antiphase. We conclude that the two dimer model is not sufficient to account for transitions to states of bound triplets, except to S_2.

Quintet states were observed by high field ESR.[14] Their extrapolated zero field energies are in the range 46–58 cm^{-1}. There are two $\mathbf{E}_1\|a$ singlet excitations at 52.3 and 53.5 cm^{-1} in this range (Table I). The quintet ($S=2$) has a $m_S=0$ spin level which has the same magnetic field dependence of energy as the $S=0$ state. However, the observed singlets at 52.3 and 53.5 cm^{-1} are not the $m_S=0$ components of the quintet. If in one $\mathbf{B}_0$ field orientation the $m_S=0$ level is infrared-active then in the 90° rotated field orientation other levels, $m_S=\pm 1$ or $m_S=\pm 2$, become active. We studied all possible $\mathbf{B}_0$, $\mathbf{E}_1$ orientations relative to crystal axes and did not find the splitting of the 52.3 and 53.5 cm^{-1} excitations in the magnetic field although they are one to two orders of magnitude more intensive than other magnetic excitations in FIR spectra.

We assigned the a-axis polarized ($\mathbf{E}_1\|a$) 43.0, 52.3, and 53.5 cm^{-1} singlet excitations to magnetic excitations because of the magnetic field and temperature dependence of their energy and intensity.[16] Whether they could be phonons activated by magnetic interactions needs a further study.

III. CONCLUSIONS

In $SrCu_2(BO_3)_2$ the ground state is not exactly a product of singlets on dimers as in the Shastry-Sutherland model, because the intradimer Dzyaloshinskii-Moriya interaction $\mathbf{d}_2$ mixes the ground singlet state with the triplet. From the observed anticrossing between $T_{0p}(+)$ and S_2 we get $d_2=1.8$ cm^{-1}. This is comparable to the interdimer DM, $d_1=0.7$ cm^{-1}, which determines the triplet state energy level zero field splitting. Both $\mathbf{d}_1$ and $\mathbf{d}_2$ determine the magnetic

field dependence of the absorption line intensities.

Although magnetic dipole singlet-triplet transitions are allowed by $\mathbf{d}_2$, the experimentally observed polarization and magnetic field dependencies of absorption line intensities are not described by this interaction. Instead, singlet-triplet transitions are allowed by the dynamic DM mechanism where the electric field component of FIR light couples to a nonsymmetric phonon, which creates the DM interaction. There are two dynamic DM mechanisms in $SrCu_2(BO_3)_2$. In one case the FIR light couples to an a-axis phonon and in the other case to a c-axis phonon. This is consistent with the calculations of Cépas and Ziman[23] who used a two dimer model in the $j_2 = 0$ limit.

The experiment also yielded information about higher triplet and singlet excitations. Several of these absorption lines are identified as electric dipole transitions. The two dimer cluster is too small to describe these transitions. Also, we had to use renormalized values of j_1 and j_2 to calculate the energy levels because the actual spin excitations are delocalized over a larger cluster. Obviously a bigger cluster is needed for proper calculation of magnetic excitations in $SrCu_2(BO_3)_2$. Nevertheless, the two dimer model gives us a good description of the one-triplet excitation.

ACKNOWLEDGMENTS

*Electronic address: roomtom@kbfi.ee

[1] H. Kageyama, K. Yoshimura, R. Stern, N. V. Mushnikov, K. Onizuka, M. Kato, K. Kosuge, C. P. Slichter, T. Goto, and Y. Ueda, Phys. Rev. Lett. **82**, 3168 (1999).

[2] K. Kodama, M. Takigawa, M. Horvatić, C. Berthier, H. Kageyama, Y. Ueda, S. Miyahara, F. Becca, and F. Mila, Science **298**, 395 (2002).

[3] H. Kageyama, M. Nishi, N. Aso, K. Onizuka, T. Yosihama, K. Nukui, K. Kodama, K. Kakurai, and Y. Ueda, Phys. Rev. Lett. **84**, 5876 (2000).

[4] B. S. Shastry and B. Sutherland, Physica B & C **108B**, 1069 (1981).

[5] S. Miyahara and K. Ueda, J. Phys.: Condens. Matter **15**, R327 (2003).

[6] C. Knetter, A. Bühler, E. Müller-Hartmann, and G. S. Uhrig, Phys. Rev. Lett. **85**, 3958 (2000).

[7] A. Koga and N. Kawakami, Phys. Rev. Lett. **84**, 4461 (2000).

[8] W. Zheng, J. Oitmaa, and C. J. Hamer, Phys. Rev. B **65**, 014408 (2001).

[9] C. H. Chung, J. B. Marston, and S. Sachdev, Phys. Rev. B **64**, 134407 (2001).

[10] A. Läuchli, S. Wessel, and M. Sigrist, Phys. Rev. B **66**, 014401 (2002).

[11] T. Munehisa and Y. Munehisa, J. Phys. Soc. Jpn. **73**, 340 (2004).

[12] O. Cépas, K. Kakurai, L. P. Regnault, T. Ziman, J. P. Boucher, N. Aso, M. Nishi, H. Kageyama, and Y. Ueda, Phys. Rev. Lett. **87**, 167205 (2001).

[13] H. Nojiri, H. Kageyama, K. Onizuka, Y. Ueda, and M. Motokawa, J. Phys. Soc. Jpn. **68**, 2906 (1999).

[14] H. Nojiri, H. Kageyama, K. Onizuka, Y. Ueda, and M. Motokawa, J. Phys. Soc. Jpn. **72**, 3243 (2003).

[15] P. Lemmens, M. Grove, M. Fischer, G. Güntherodt, V. N. Kotov, H. Kageyama, K. Onizuka, and Y. Ueda, Phys. Rev. Lett. **85**, 2605 (2000).

[16] T. Rõõm, U. Nagel, E. Lippmaa, H. Kageyama, K. Onizuka, and Y. Ueda, Phys. Rev. B **61**, 14342 (2000).

[17] C. Knetter and G. S. Uhrig, Phys. Rev. Lett. **92**, 027204 (2004).

[18] A. Zorko, D. Arčon, H. van Tol, L. C. Brunel, and H. Kageyama, Phys. Rev. B **69**, 174420 (2004).

[19] S. Miyashita and A. Ogasahara, J. Phys. Soc. Jpn. **72**, 2350 (2003).

[20] K. Sparta, G. J. Redhammer, P. Roussel, G. Heger, G. Roth, P. Lemmens, A. Ionescu, M. Grove, G. Güntherodt, F. Hüning *et al.*, Eur. Phys. J. B **19**, 507 (2001).

[21] K.-Y. Choi, Y. G. Pashkevich, K. V. Lamonova, H. Kageyama, Y. Ueda, and P. Lemmens, Phys. Rev. B **68**, 104418 (2003).

[22] B. Wolf, S. Zherlitsyn, S. Schmidt, B. Lüthi, H. Kageyama, and Y. Ueda, Phys. Rev. Lett. **86**, 4847 (2001).

[23] O. Cépas and T. Ziman, Phys. Rev. B **70**, 024404 (2004).

[24] H. Kageyama, K. Onizuka, T. Yamauchi, and Y. Ueda, J. Cryst. Growth **206**, 65 (1999).

[25] T. Rõõm, D. Hüvonen, U. Nagel, Y.-J. Wang, and R. K. Kremer, Phys. Rev. B **69**, 144410 (2004).

[26] Weak 52.3 and 53.5 cm^{-1} lines are present in $\mathbf{E}_1 \| \mathbf{c}$ spectra because the crystal was misaligned relative to the light $\mathbf{k}$ vector; that created a small in-plane $\mathbf{E}_1$ component. As estimated from the residual intensity of the 52.3 and 53.5 cm^{-1} lines in $\mathbf{E}_1 \| \mathbf{c}$ polarization the $\mathbf{k}$ vector was out of the (ab) plane by $12 \pm 2°$. The same applies to the $\mathbf{B}_0$ field in Faraday configuration, $\mathbf{B}_0 \| \mathbf{k}$. Misalignment of $9 \pm 1°$ is calculated from the splitting of the triplet components, Fig. 6.

[27] L. Shekhtman, O. Entin-Wohlman, and A. Aharony, Phys. Rev. Lett. **69**, 836 (1992).

[28] L. Shekhtman, A. Aharony, and O. Entin-Wohlman, Phys. Rev. B **47**, 174 (1993).

[29] G. Jorge, R. Stern, M. Jaime, N. Harrison, J. Bonca, S. E. Shawish, C. Batista, H. Dabkowska, and B. Gaulin, cond-mat/0309534 (unpublished).

[30] S. Miyahara, F. Mila, K. Kodama, M. Takigawa, M. Horvatic, C. Berthier, H. Kageyama, and Y. Ueda, J. Phys.: Condens. Matter **16**, S911 (2004).